Wear 530-531 (2023) 205074

Contents lists available at ScienceDirect

Wear

journal homepage: www.elsevier.com/locate/wear

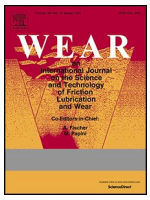

A fast version of 'CONTACT' for normal problem calculations

Juan Giner-Navarro [a], Jorge Gómez-Bosch [a], Asier Alonso [b], Luis Baeza [a,*]

[a] I2MB, Universitat Politècnica de València, Valencia, Spain
[b] CAF I+D, Beasain, Spain

ARTICLE INFO

Keywords:
Non-Hertzian contact
Normal contact
Wheel-rail contact
CONTACT software
NORM algorithm

ABSTRACT

In its different versions, the CONTACT method developed by Prof. Kalker is the primary reference in wheel-rail contact mechanics. Despite adopting simplifications associated with the elastic behaviour of the solids and being a non-conformal contact theory, CONTACT provides precise solutions for most wheel-rail contact conditions, with lower computational and modelling costs than other numerical methods such as Finite Elements. Nevertheless, the computational cost of CONTACT is still too high for its implementation in dynamic simulation.

The present work proposes a fast and accurate wheel-rail contact method for normal problems based on Kalker's CONTACT algorithm. Dissimilarly to CONTACT, the new method formulates the normal traction distribution through a suitable basis, which reduces the dimension of the problem. This method is able to faithfully reproduce the contact patch and the normal traction distribution, even when the yaw angle of the wheelset is non-zero. Results obtained with this method are compared with the ones calculated with CONTACT, and errors about 0.05% are obtained in normal contact forces, with a reduction on the computation cost between 30 and 60 times.

1. Introduction

Among all the theories that allow to obtain a solution to the wheel-rail contact problem according to the normal direction, CONTACT (in its NORM variant) [1] is the reference in terms of precision when it comes to analysing the non-conformal contact between two surfaces that do not satisfy Hertzian contact conditions. The adoption of Hertzian contact assumption produces significant deviations when realistic conditions are simulated, both at the local contact level and in the global dynamics of the vehicle [2]. The high computational cost of each calculation using CONTACT has however limited its implementation fundamentally to offline calculations since its development during the 1980s. Even though contributions based on the adoption of more efficient methodologies for solving the associated mathematical problem [3] and, above all, the improvement of computers, have made it possible for CONTACT to be implemented in simulation of railway vehicle dynamics [4], most of the works in the literature (see reviews [5,6]), as well as commercial software [7], make use of simplified models of wheel-rail normal contact at the present time.

The first simplified models that tried to solve the non-Hertzian problems provided an approximation to the normal traction distribution and the contact area shape, which are based on Hertz formulae. This strategy was also used to find a solution to the multi-contact problem through an equivalent ellipse [8,9]. In Ref. [10], Alonso *et al.* contributed with a model in which the normal traction distribution in the contact area is assumed to be the square root of the distance between the wheel and the rail undeformed surfaces. This function is corrected through a factor derived from the maximum traction obtained from Hertz model. The method (called SRST) produces good agreement with CONTACT when the contact point is the tangency between two arcs of the rail profile, and the wheel geometry is a cone. The same problem is subject of study in Ref. [11], in which the contact area is generated by combining several ellipses obtained through the Hertz formulation, from the different combinations of radii of curvature and by imposing continuity. The method is applied to a limited number of cases, obtaining results that, according to the authors, are accurate. In Ref. [12], the semi-Hertzian method is extended in order to consider wheelset yaw angles.

Linder [13] introduces the virtual penetration method. This technique is based on the fact that the actual contact area is similar to the penetration area of the undeformed rail and wheel surfaces but of a smaller dimension. For this, it is assumed that the contact area coincides with the penetration area, considering an approach smaller than the real one (between 50 and 60%). In the method presented in Ref. [13], the

* Corresponding author. Edificio 5E, Ing. Mecánica. Universidad Politécnica de Valencia Camino de Vera s/n, 46022, Valencia, Spain.
E-mail address: baeza@mcm.upv.es (L. Baeza).

https://doi.org/10.1016/j.wear.2023.205074
Received 26 February 2023; Received in revised form 25 July 2023; Accepted 31 July 2023
Available online 3 August 2023

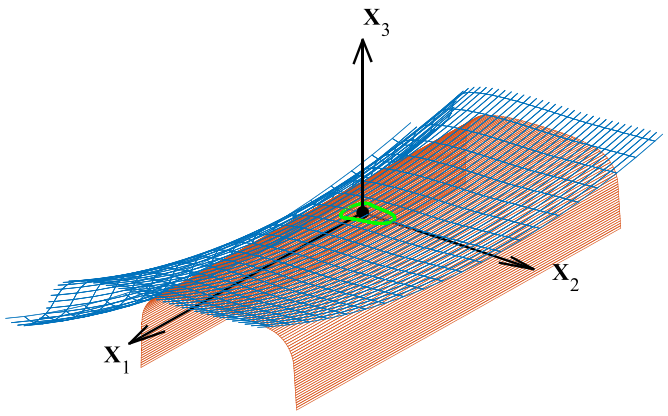

Fig. 1. Frame of reference adopted for the contact.

Table 1
Model data.

Rail profile	UIC60
Rail inclination	1/40
Track gauge	1435 mm
Wheel profile	S1002
Wheel diameter	900 mm
Distance between plane of rolling radii	1500 mm
Vertical load per wheelset	200 kN
Wheel and rail Young modulus	$2.1{\cdot}10^{11}$ N/m^2
Wheel and rail Poisson ratio	0.3
Nr. of elements in the mesh	60 × 60

contact patch is obtained by applying a constant scaling factor equal to 0.55. Once the contact patch is obtained, it is divided then into strips along the rolling direction. Each of these strips is assigned to an equivalent ellipse, with constant lateral semi-axis that is equal to half the lateral size of the contact patch. The longitudinal semi-axis is calculated so that the strip fits into the resulting equivalent ellipse. Normal tractions over these strips are calculated according to Hertz theory with the equivalent ellipse parameters of each strip. Ayasse and Chollet improved Linder's method through their code Stripes [14]. In Stripes, the semi-axes of equivalent ellipses of each strip are calculated compensating the curvatures at the centre of each strip.

In Ref. [15], it is proposed a method that assumes that the displacements associated with the elastic deformations correspond to quadrics whose coefficients, for each lateral position, are calculated by imposing the formulation of the size of the ellipse provided by the Hertzian contact model. The contact patch is assumed to be the virtual penetration area. The program that implements this model (called Analyn) is very efficient from a computational point of view. Compared with Stripes [14], it achieves better results, but significant differences appear with respect to CONTACT. Analyn extends the calculation of surface damage in Ref. [16] and the calculation of wheel wear in Ref. [17], in which a modification is proposed to consider yaw angle for the wheelset.

In [18], Kik and Piotrowski develop a Hertz-independent method based on virtual penetration. Once the contact area is known, the Boussinesq integrals are calculated by imposing that the displacement due to the deformations is half-distance between the undeformed surfaces. From this approach, it is obtained a formulation that depends on integrals that have to be calculated numerically. This procedure is fast enough to be implemented in the simulation of low-frequency vehicle dynamics [19]. Several authors have proposed enhancements of Kik and Piotrowski method, such as Ref. [20] (which considers the wheelset yaw angle), Ref. [21] (that introduces an amendment that increases the algorithm stability), and Ref. [22] (that increases the precision of the method when the vehicle negotiates sharp curves).

Different contact models, especially those based on virtual penetration, are frequently benchmarked in the literature. In Ref. [23], results from CONTACT are compared with Stripes [14], Kik and Piotrowski method [18], and Linder's [13]. The comparison shows a poor fit with the results provided by CONTACT, especially regarding the contact traction distribution. A wider benchmark (which compares CONTACT with Hertz solution [24], Stripes, Kik and Piotrowski model, Linder model, and Analyn [15]) can be found in Ref. [25]. In general, the agreement of the tested methods to CONTACT is poor, having Analyn the more accurate results. The same group carries out a similar study with identical conclusions for the case in which the wheelset is running on a S&C panel [26].

Another family of normal contact theories that implement the elastic behaviour of solids as infinite half-spaces (Exact Theories according to the Kalker's classification [27]) corresponds to those that assume an elliptical traction distribution according to the rolling direction. The various published methods differ according to the technique used to perform the integration of the Boussinesq integral. Nielsen [28] was able to transform this integral equation into an algebraic equation through polynomials that approximate the traction distribution in a 2D case (the contact area only considers the rolling coordinate), expressing the normal contact as a system of algebraic equations. In Ref. [29], the Boussinesq integral is calculated through Gauss quadrature; it must be pointed out that the Boussinesq integrals are not integrable in the conventional sense (because the integrand is singular in the integration domain), and numerical integration should not be applied in such cases.

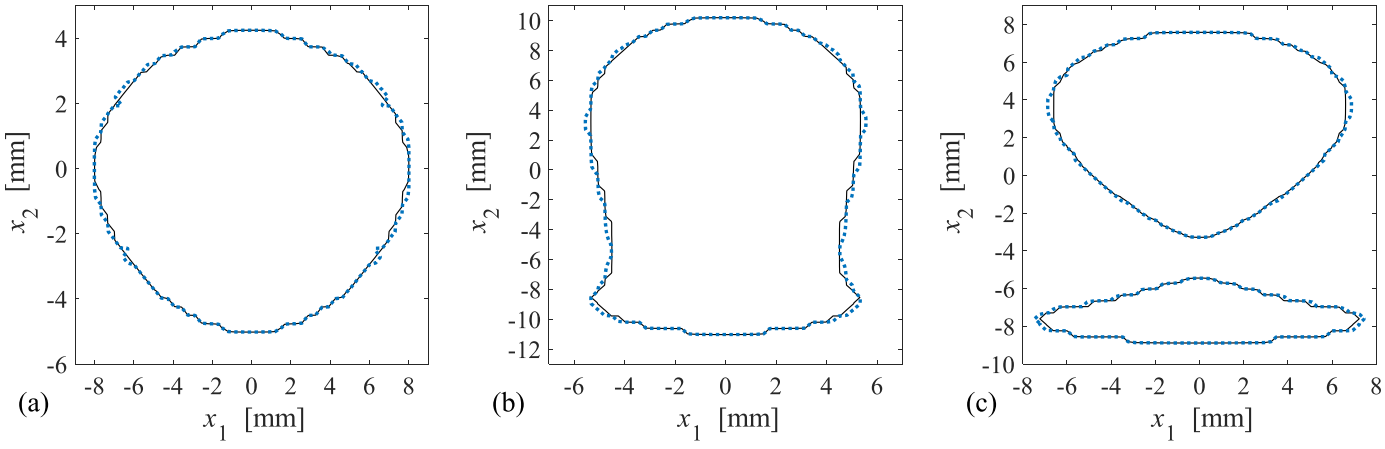

Fig. 2. Contact area shape for different wheelset lateral displacements: (a) conditions close to Hertzian ($y = 4$ mm); (b) non-Hertzian contact conditions ($y = 0$ mm); (c) multi-contact conditions ($y = 5$ mm). Solid line corresponds to CONTACT and dotted line corresponds to the proposed model.

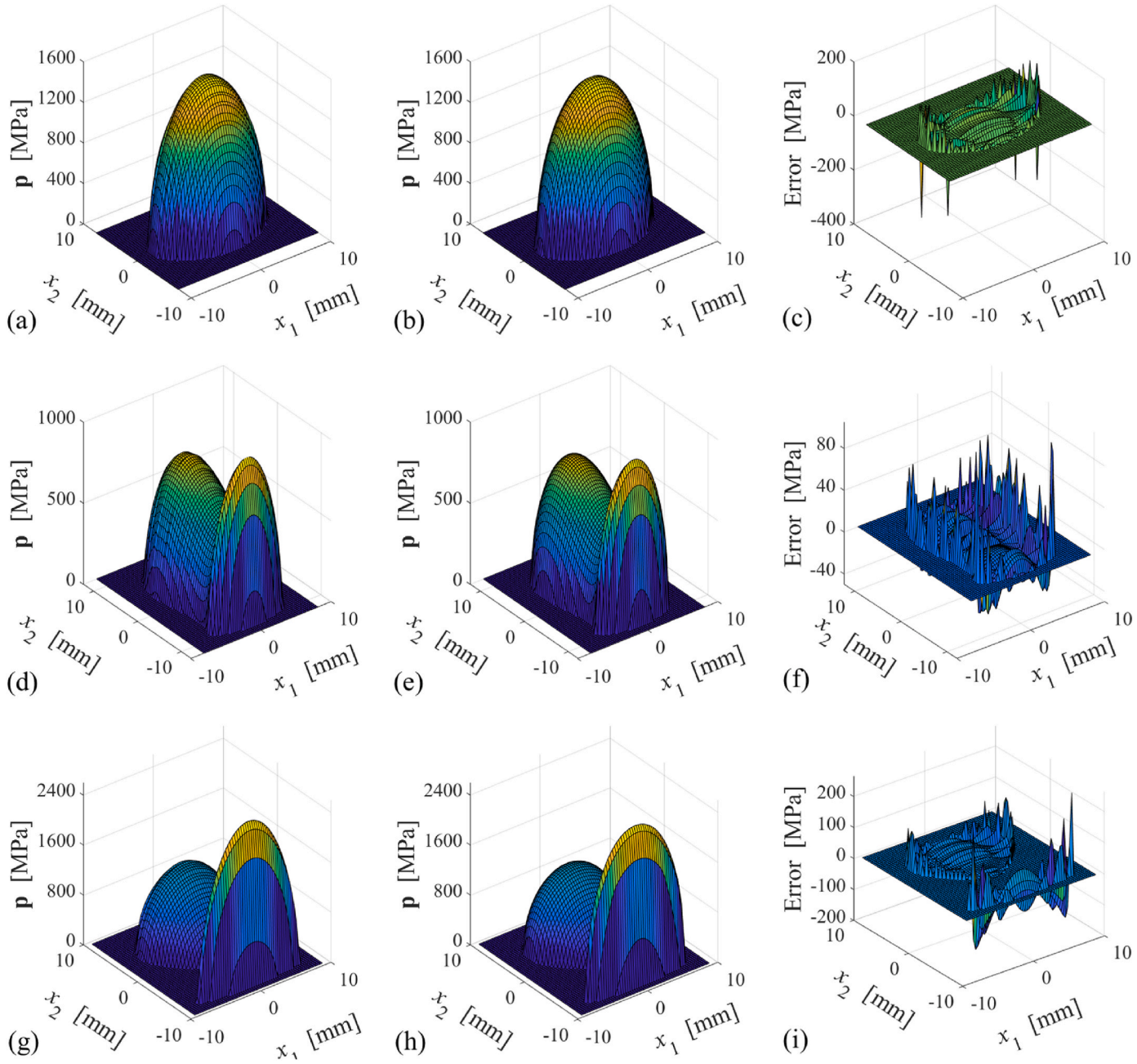

Fig. 3. Normal traction distribution for different wheelset lateral displacements: (a) Hertzian contact conditions ($y = 4$ mm), elliptical basis; (b) Hertzian contact condition, CONTACT ($y = 4$ mm); (c) absolute error associated with the elliptical basis ($y = 4$ mm); (d) non-Hertzian contact conditions ($y = 0$ mm), elliptical basis; (e) non-Hertzian contact conditions, CONTACT ($y = 0$ mm); (f) absolute error associated with the elliptical basis ($y = 0$ mm); (g) multi-contact conditions ($y = 5$ mm), elliptical basis; (h) multi-contact conditions, CONTACT ($y = 5$ mm); (i) absolute error associated with the elliptical basis ($y = 5$ mm).

Reusner and Qazi solved this difficulty brilliantly. In Ref. [30], the integral is reformulated by means of elliptic integrals; and Ref. [31] reformulates the Boussinesq integrand producing a sum of two integrals, one of them has a closed form solution, and the other is integrable and can be solved by quadrature. These methods have not mathematically proven convergence [1], while the calculation of the elastic influence coefficients is more complex and they cannot consider the asymmetric traction distribution produced by the yaw angle of the wheelset. However, its physical principle can be adopted in the formulation of CONTACT to combine its precision, reliability and versatility, thus reducing the computational cost.

The present work proposes a modification in the formulation of the CONTACT method for solving the normal contact problem, through which a substantial reduction in computational cost is achieved with hardly any reduction in precision. The method is based on the fact that the traction distribution according to the rolling direction (in each strip of the mesh when CONTACT discretisation is considered) has an approximately elliptical shape. Therefore, the distribution of tractions in each strip can be formulated through a suitable function basis that depends on a reduced number of parameters. The paper develops the method by means of two basis families: one of them produces accurate results when the yaw angle of the wheelset is close to zero, and the other one allows to calculate the normal traction distribution even if the yaw angle and the lateral displacement of the wheelset are large. The proposed algorithm computes the total contact force with errors less than 0.1%, calculating contact areas identical to those obtained by CONTACT

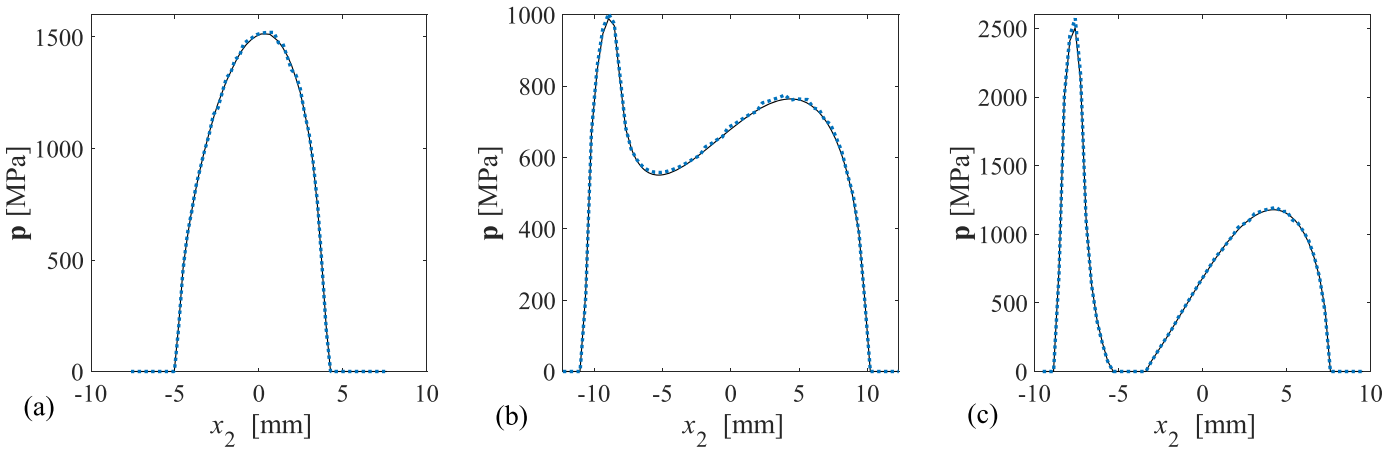

Fig. 4. Normal traction distribution over the $x_1 = 0$ strip for different wheelset lateral displacements: (a) Hertzian contact conditions ($y = 4$ mm); (b) non-Hertzian contact conditions ($y = 0$ mm); (c) multi-contact conditions ($y = 5$ mm). Solid line corresponds to CONTACT and dotted line corresponds to the proposed model.

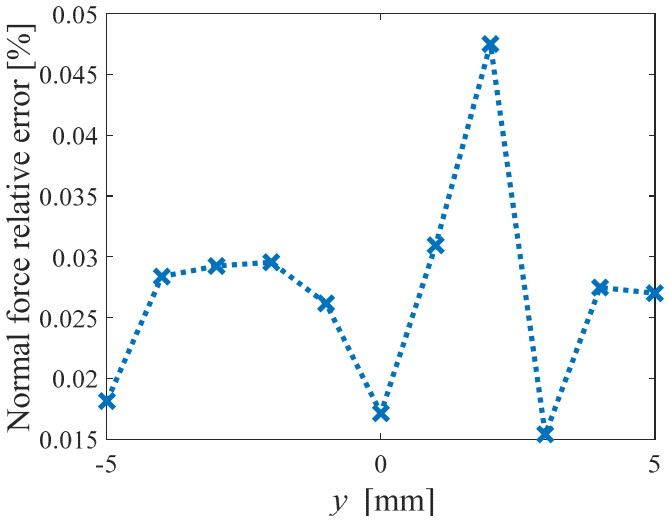

Fig. 5. Normal force relative error vs. wheelset lateral displacement y.

Table 2
Error in the normal contact force [%] as function of the polynomial grade for different wheelset lateral displacements y and yaw angles ψ.

Grade	$y = 4, \psi = 0°$	$y = 0, \psi = 0°$	$y = 5, \psi = 0°$	$y = 0, \psi = 1°$	$y = 0, \psi = 2°$
$g = 2$	0.121	0.237	0.047	0.120	0.102
$g = 3$	0.121	0.237	0.047	0.139	0.134
$g = 4$	0.031	0.030	0.041	0.040	0.042
$g = 5$	0.031	0.030	0.041	0.040	0.042
$g = 6$	0.031	0.030	0.040	0.040	0.041
$g = 7$	0.031	0.030	0.040	0.040	0.041
$g = 8$	0.030	0.029	0.040	0.039	0.041
$g = 9$	0.030	0.029	0.040	0.039	0.041
$g = 10$	0.030	0.029	0.040	0.039	0.041

and allowing the calculation of asymmetric traction distributions due to the yaw angle of the wheelset.

2. Proposed model

In the present work, a frame of reference $\mathbf{X_1X_2X_3}$ is adopted (see Fig. 1), whose origin is the centre of the potential contact area, obtained from the solution of the geometrical contact problem. The $\mathbf{X}_1$-axis corresponds to the rolling direction, the $\mathbf{X}_3$-axis is normal to the contact area (being the positive direction towards the wheel), and the $\mathbf{X}_2$-axis is associated with the lateral direction (positive according to a right-handed frame of reference). It is considered that the rail and wheel undeformed surfaces interpenetrate, which corresponds to the usual conditions for calculating the contact problem in dynamic simulation programs. According to CONTACT, the potential contact area is divided into a regular mesh of rectangles in which the normal traction is assumed to be constant in each element of the mesh. The CONTACT (NORM) method is based on solving the following equation:

$$\mathbf{h} = \mathbf{C}\,\mathbf{p}, \tag{1}$$

where $\mathbf{h}$ is the vector that contains the distance between the rail and wheel undeformed surfaces in contact for each element, $\mathbf{C}$ is a full Toeplitz matrix with the elastic influence coefficients, and $\mathbf{p}$ orders the unknown normal tractions of the elements in contact. Therefore, to obtain the contact area and the normal traction distribution, Eq. (1) is solved iteratively, checking which elements present a normal traction value equal or lower than zero, and discarding them for the next iteration until convergence is achieved [1].

The proposed algorithm is based on the fact that the traction distribution according to the $\mathbf{X}_1$-direction (in each strip of the mesh) has an approximately elliptical shape. Therefore, the distribution in each strip can be formulated through a suitable basis that depends on a reduced number of parameters. Assuming that this basis is formulated by means of an ellipse, the normal traction p_{es} in the e-th element of the mesh found in the s-th strip can be written as follows:

$$p_{es} \approx \alpha_{0s} + \alpha_{1s}\sqrt{1 - \left(\frac{x_{es}}{L_s}\right)^2}, \tag{2}$$

being x_{es} the coordinate according to the rolling direction of the e-th element in the s-th strip, L_s the semi-axis of the strip in the rolling direction, and α_{gs} the coefficient of order g corresponding to the s-th strip. To detect the elements that should not be included in the contact area, this base equation is able to admit a solution that provides a negative value of traction in such elements (they are at the edge of the contact area) through α_{0s}. In the last calculation through the NORM algorithm

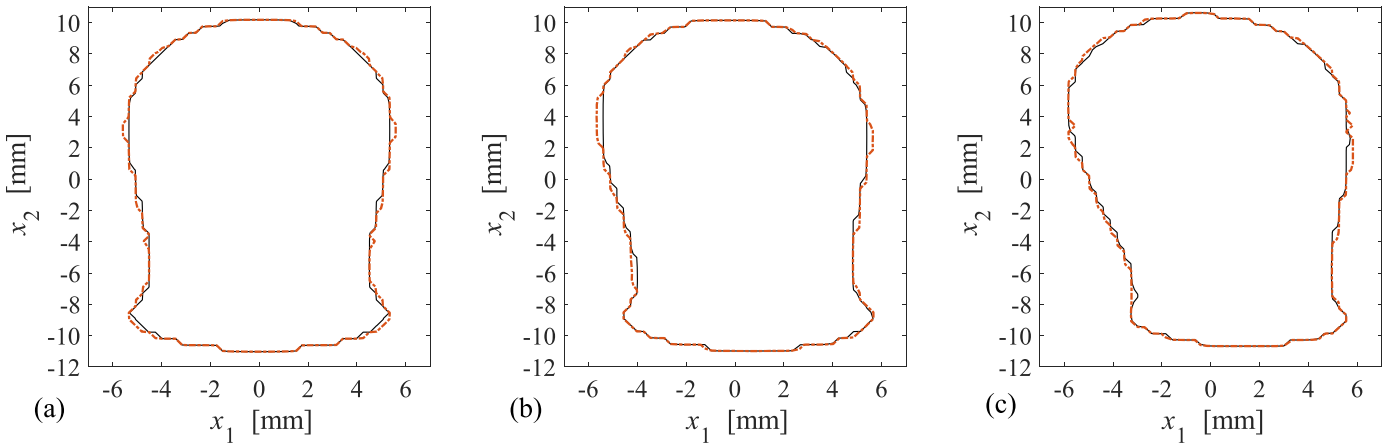

Fig. 6. Contact area shape for different wheelset yaw angles. (a) $\psi = 0°$; (b) $\psi = 1°$; (c) $\psi = 2°$. Solid line corresponds to CONTACT and dash-dotted line corresponds to polynomial basis of $g = 4$.

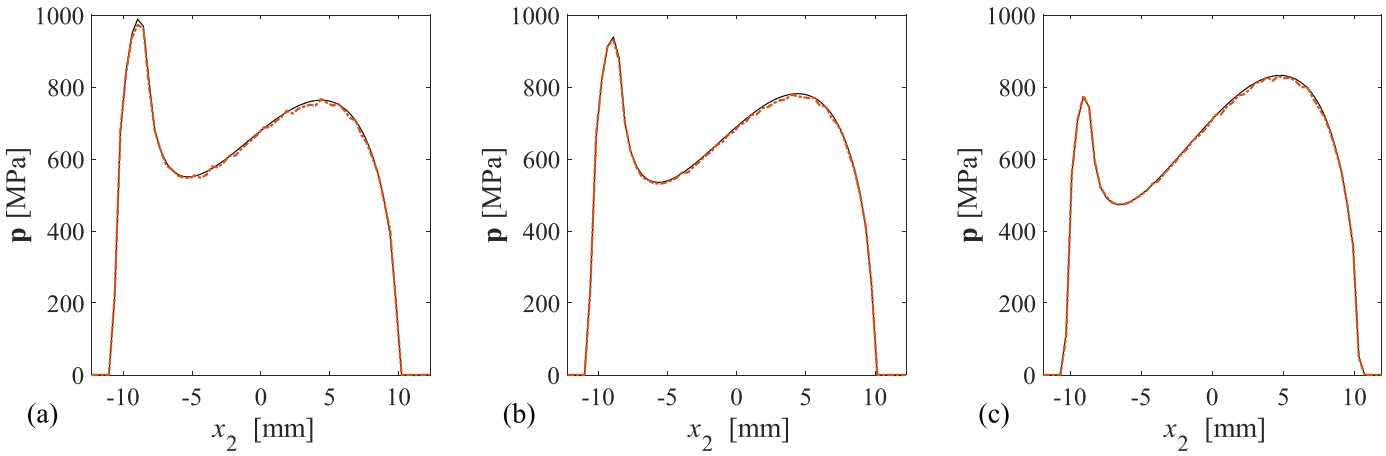

Fig. 7. Normal traction distribution over the $x_1 = 0$ strip for different wheelset yaw angles: (a) $\psi = 0°$, (b) $\psi = 1°$; (c) $\psi = 2°$. Solid line corresponds to CONTACT and dash-dotted line corresponds to polynomial basis of $g = 4$.

[1], the constant value is practically zero, so this parameter can also be used to know that the right solution has been reached. According to this approximation, the traction vector $\mathbf{p}$ can be written as

$$\mathbf{p} \approx \mathbf{A}\,\boldsymbol{\alpha}, \tag{3}$$

where in the vector $\boldsymbol{\alpha}$ the coefficients α_{gs} are stored, and $\mathbf{A}$ is a matrix that depends on the mesh coordinates x_{es} and the strip lengths L_s (as the contact area is known in each calculation, x_{es}, L_s and, consequently, $\mathbf{A}$ are known). Note that the dimension of $\boldsymbol{\alpha}$ is 2 times the number of mesh strips N_s. The appendix of this paper presents an example of how matrix $\mathbf{A}$ is built for a mesh with a few elements, which helps to illustrate the method.

After substituting the result of Eq. (3) in (1), and pre-multiplying the resulting equation by $\mathbf{A}^{\mathrm{T}}$ (being the superscript T the transposition of the matrix), it turns out

$$\mathbf{A}^{\mathrm{T}}\,\mathbf{h} = \mathbf{A}^{\mathrm{T}}\,\mathbf{C}\,\mathbf{A}\,\boldsymbol{\alpha}, \tag{4}$$

and from Eqs. (3) and (4),

$$\mathbf{p} = \mathbf{A}\left(\mathbf{A}^{\mathrm{T}}\,\mathbf{C}\,\mathbf{A}\right)^{-1}\left(\mathbf{A}^{\mathrm{T}}\,\mathbf{h}\right). \tag{5}$$

Since α_{0s} and α_{1s} are the two unknown variables per strip, Eq. (4) corresponds to a linear system of dimension $2N_s$, being N_s the number of strips, in general much smaller than the original dimension of Eq. (1) that corresponds to the number of elements N in the contact area.

Despite the reduction of the problem dimension brought by this basis, this method is unable to faithfully reproduce the contact area when there exists a non-null wheelset yaw angle ψ. When this occurs, plane $\mathbf{X_2X_3}$ is no longer a symmetry plane of the normal traction distribution and, due to the symmetry of the basis used in Eq. (2), only symmetric normal traction distributions can be obtained. To deal with this issue, a polynomic normal traction distribution is proposed instead of an elliptical one:

$$p_{es} \approx \sum_{j=0}^{g} \beta_{js}\, x_{es}^{j}, \tag{6}$$

being now g the grade of the polynomial and β_{js} the polynomial coefficient of order j corresponding to the s-th strip of the mesh. Following the same procedure than the one described for the elliptic basis, $\mathbf{p}$ for the polynomial approximation can be written as

$$\mathbf{p} \approx \mathbf{B}\,\boldsymbol{\beta}, \tag{7}$$

where $\boldsymbol{\beta}$ is the vector that contains the polynomial coefficients. The appendix of this paper presents an example of how matrix $\mathbf{B}$ is built for a mesh with a few elements.

Following a procedure analogous to that presented for the elliptical basis, the following system is obtained:

$$\mathbf{B}^{\mathrm{T}}\,\mathbf{h} = \mathbf{B}^{\mathrm{T}}\,\mathbf{C}\,\mathbf{B}\,\boldsymbol{\beta}. \tag{8}$$

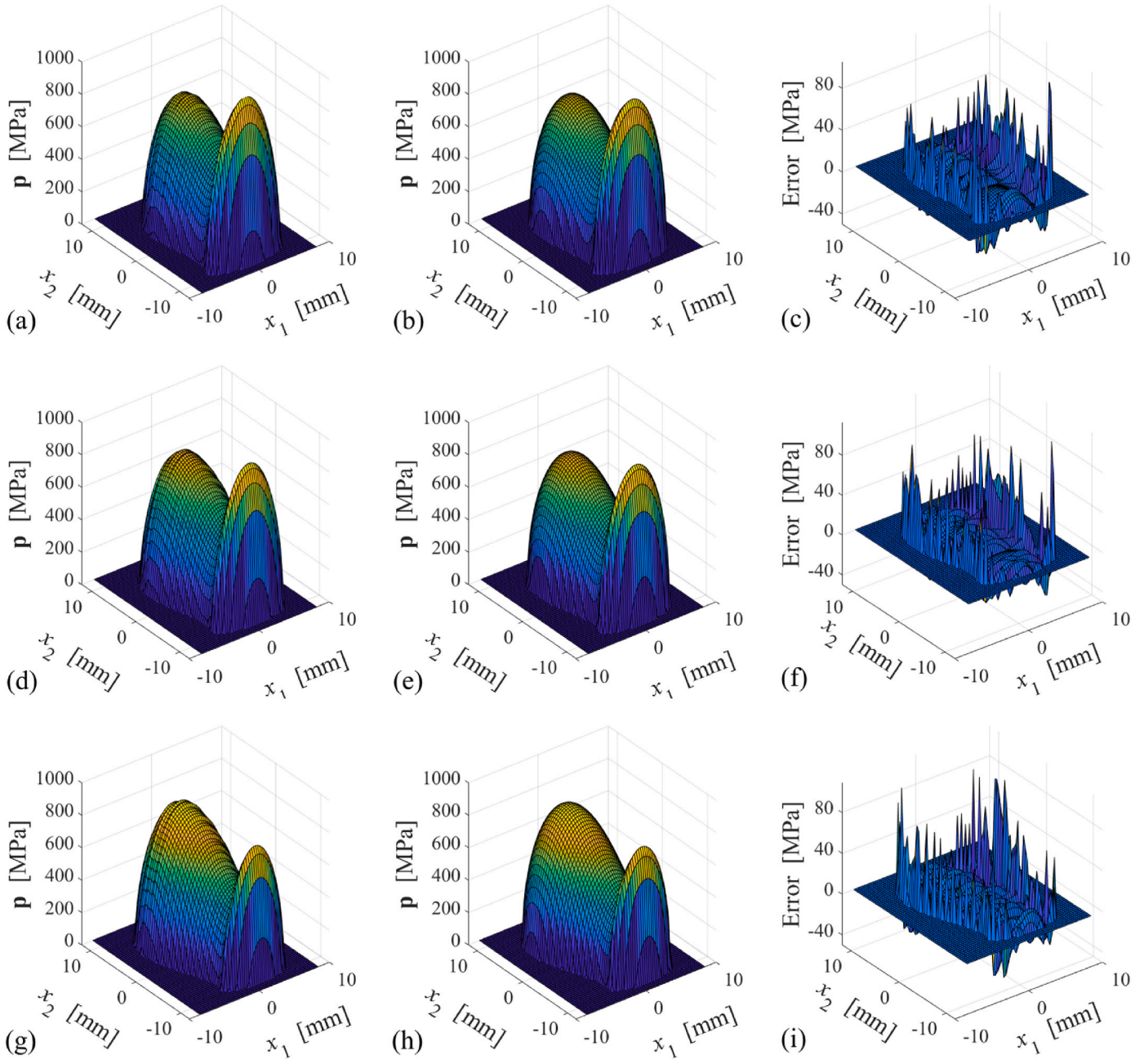

Fig. 8. Normal traction distribution for different wheelset yaw angles: (a) polynomial basis of grade $g = 4$ ($\psi = 0°$); (b) CONTACT ($\psi = 0°$); (c) absolute error associated with the polynomial basis ($\psi = 0°$); (d) polynomial basis of grade $g = 4$ ($\psi = 1°$); (e) CONTACT ($\psi = 1°$); (f) absolute error associated with the polynomial basis ($\psi = 1°$); (g) polynomial basis of grade $g = 4$ ($\psi = 2°$); (h) CONTACT ($\psi = 2°$); (i) absolute error associated with the polynomial basis ($\psi = 2°$).

For this basis, the dimension of the problem increases to $(g + 1)N_s$, but is much smaller than the original dimension of the problem. The normal traction distribution is finally computed through the polynomial basis as follows:

$$\mathbf{p} = \mathbf{B}\left(\mathbf{B}^{\mathrm{T}}\,\mathbf{C}\,\mathbf{B}\right)^{-1}\left(\mathbf{B}^{\mathrm{T}}\,\mathbf{h}\right). \tag{9}$$

3. Results

This method is proposed to be a fast alternative to Kalker's CONTACT (NORM) algorithm [1]. To prove its validity, results obtained with the proposed methods are confronted to the ones given by CONTACT as reference solution. To further compare the calculation performance under the same computational conditions, both elliptical and polynomial methods, as well as the CONTACT algorithm, have been programmed in a C code that implements the same numerical methods for solving systems of linear equations.

In order to perform all these calculations, it has been chosen a test-set compatible with realistic values of a vehicle running on a track (see Table 1), together with a set of plausible wheelset lateral displacements y and yaw angles ψ to simulate realistic circulation conditions. To this end, the undeformed distance between the wheel and the rail is calculated for a free wheelset under frictionless static conditions. In these calculations, the lateral displacement y and the yaw angle ψ are prescribed, and the vertical load is applied in the wheelset centre of mass (COM). The contact topology is obtained using a method based on the intersections between cones and lines proposed in Ref. [32], which allows determining the distance $\mathbf{h}$ between the rail and wheel undeformed

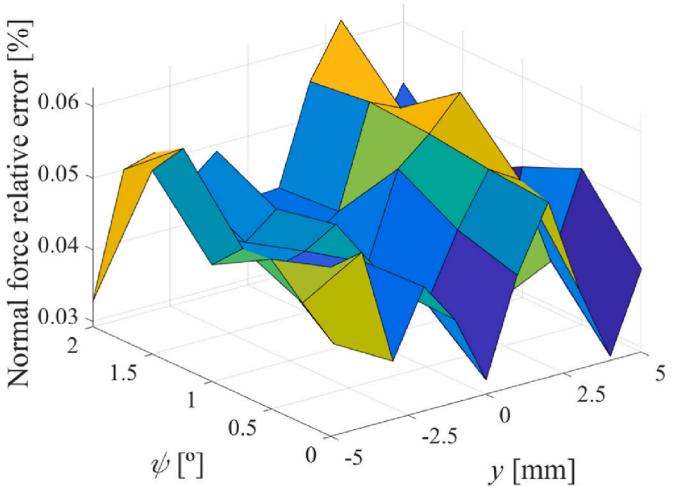

Fig. 9. Normal force relative error for different wheelset lateral displacements y and yaw angles ψ.

surfaces. This distance is used as input to solve the normal contact problem using the Kalker's CONTACT (NORM) algorithm [1]. A Newton-Raphson scheme is used for the iteration process that found the COM vertical position z and the roll angle φ that determine the position of the wheelset on the rails for static equilibrium conditions. With the wheelset position as input data, the normal contact forces in both wheel-rail contact areas are computed through both proposed bases.

3.1. Influence of the wheelset lateral displacement

In order to analyse the accuracy of the method under different contact conditions, the contact area shape and the normal traction distribution are computed for different wheelset lateral displacements. Fig. 2 gathers the contact shapes simulated through CONTACT and the elliptical approach for three different lateral displacements: $y = 4$ mm (conditions close to Hertzian contact), $y = 0$ mm (non-Hertzian contact conditions), and $y = 5$ mm (multiple contact). The calculated areas through the exact and the proposed method almost coincide as seen in the figure.

For the same conditions, the normal traction distribution throughout the whole contact patch is plotted in Fig. 3 for both methods. It can be observed that the traction over each strip is close to an ellipse for all the cases studied, given that no appreciable differences in the distribution exist between CONTACT and the results obtained with the elliptical basis. The figure includes the absolute errors between both models, in which the maximum discrepancies are found on the border of the

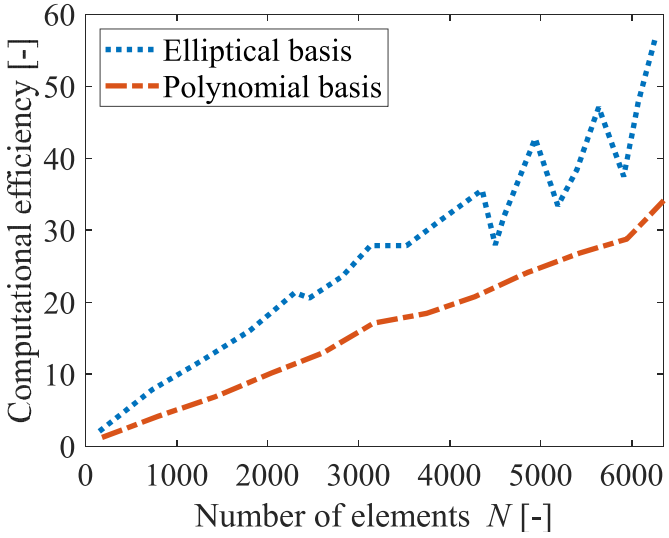

Fig. 11. Computational efficiency as a function of the number of elements of the mesh N.

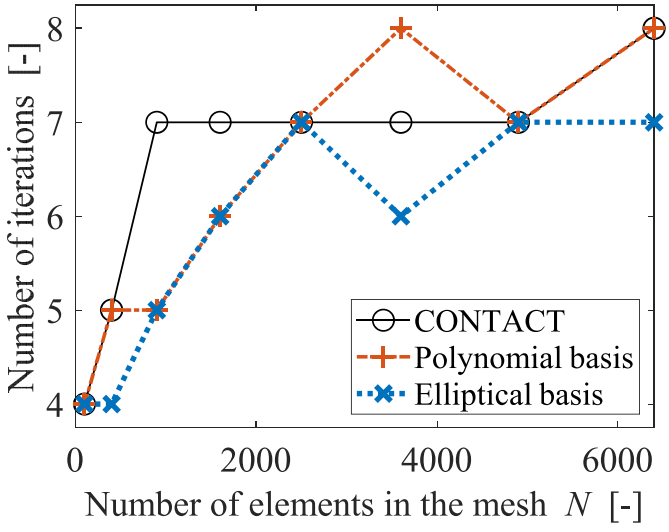

Fig. 12. Number of iterations necessary for the convergence of the method as a function of the number of elements of the mesh N.

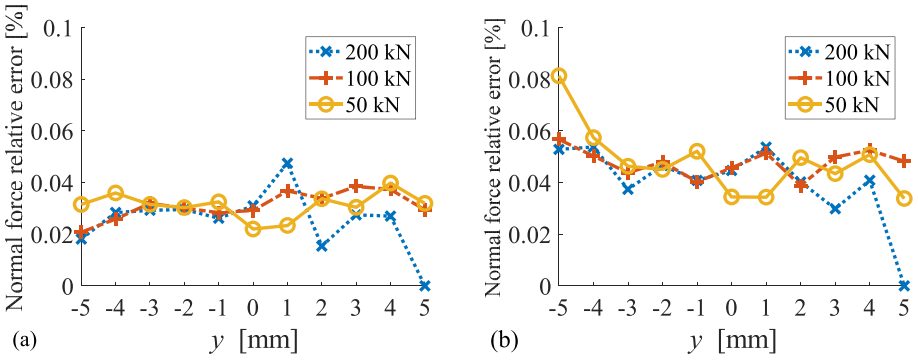

Fig. 10. Normal force relative error for different y values and normal load values. (a) Elliptical basis; (b) polynomial basis of grade $g = 4$.

contact area, where it is checked whether the extreme elements of the strip are or not in contact. Carrying out a detailed analysis of the differences in the results, Fig. 4 shows the traction distribution over the strip $x_1 = 0$ for both models, which are almost coincident. Fig. 5 presents the relative errors of the total normal force for the three lateral displacements previously evaluated. For all the studied cases, the errors are below 0.05%.

3.2. Influence of the wheelset yaw angle

One advantage of the proposed method with respect to other theories relies on the capability to obtain accurate results even when the wheelset yaw angle is different from zero. To prove the accuracy of the method under these conditions, similar studies than the case presented above are carried out for a polynomial basis. In order to select the lowest grade g that guarantees a good precision with respect to the normal contact force calculated by CONTACT as reference solution, approximations from $g = 2$–10 has been performed to evaluate the errors (see Table 2). It should be noted that, in the strips near the leading and trailing edges, it may happen that the number of elements in contact is smaller than the polynomial grade used in the approximation, then requiring that the normal contact is solved in these strips using CONTACT. This partly explains the residual errors to which the simulations with increasing polynomial grade converge. It is concluded that $g = 4$ provides a significant reduction of the errors with respect to $g = 3$ for all the combinations of wheelset lateral displacements y and yaw angles ψ simulated. These errors hardly decrease beyond this grade (it could be observed in the fourth or fifth decimal in %), hence there is no need to use higher polynomial grades to guarantee the accuracy of the method, with $g + 1 = 5$ unknowns β_{js} per strip according to Eq. (6).

Fig. 6 shows the computed shape of the contact area versus CONTACT for three different yaw angles. The results give slight variations for the analysed cases, showing that the approximation is capable to accurately represent the contact shape no matter the value of the yaw angle.

Fig. 7 presents the normal traction distribution over the $x_1 = 0$ strip for this polynomial approach, with results that practically overlaps the ones provided by the exact method for three different yaw angles: $\psi = 0°$, $\psi = 1°$ and $\psi = 2°$. Fig. 8 shows the normal traction distribution for the same three different yaw angle values of the wheelset. The figure confronts again the results for the polynomial and the exact method, which are practically the same at first glance even when there exists yaw angle. It also includes the absolute error associated with the normal traction distribution calculated through the proposed model, with higher deviations again in the first and last element of the strip (below 85 MPa in all cases). In order to delve into the deviations between both traction distributions, Fig. 9 gathers the relative errors of the total contact force for different values of the lateral displacement and the yaw angle (the latter parameter is only presented in positive values since the errors obtained are symmetric for the negative angles). As observed, errors are about 0.05% for all the cases studied.

3.3. Influence of the normal load

As the contact conditions may be affected by the normal load (and thus the normal traction distribution), it is proposed to analyse the influence of the normal load on the wheelset in order to prove the validity of the proposed method to be applied in railway dynamics for different purposes. Fig. 10 gathers the relative error that each approach (elliptical and polynomial) gives for the total normal force considering different vertical loads and wheelset lateral displacements, showing errors below 0.1% regardless the vertical load applied to the wheelset.

Despite both approximations present low errors for all the studied cases, the ones obtained with the elliptical basis are generally lower than the polynomial one as this basis fits better to the normal traction distribution obtained with CONTACT over a strip. This conclusion reinforces the idea that the exact distribution is very close to the elliptical shape, hence a model with an elliptic basis is more accurate than a polynomial one.

3.4. Computational efficiency

The computational efficiency is measured as the ratio between the calculation times consumed by CONTACT and the proposed method. Fig. 11 shows the computational efficiency for each basis as a function of the number of elements of the contact mesh N. As the elliptical method computes fewer unknowns (2 coefficients per strip versus 5 polynomial coefficients when $g = 4$), the subsequent larger reduction of the problem dimension leads to a better computational performance, being up to 60 times faster than CONTACT, whereas the polynomial method is about 35 times faster. Fig. 12 presents the number of iterations needed by the algorithm to reach convergence, showing that the elliptical approximation needs less iterations even than CONTACT does in most of the analysed cases.

4. Conclusions

In this work, a methodology based on Kalker's CONTACT (NORM version) program is presented to solve the normal contact problem faster than the original method with scarce accuracy loss. The enhance of the computational efficiency is achieved due to the reduction of the number of unknowns through the introduction of suitable bases to represent the normal traction distribution. The chosen bases implemented in the present work are an elliptical and a polynomial function of grade 4, whose results have been compared with the contact area shape, normal traction distribution and computational times provided by CONTACT.

The elliptical approach performs up to 60 times faster than CONTACT original algorithm but, despite its lower errors, it is limited by its lack of capability to model the normal contact with the presence of a large yaw angle. The need of a different approach led to implement a polynomial approximation, which is able to faithfully reproduce the contact area shape and traction distribution no matter the value of the yaw angle with errors in the total normal force about 0.05% with respect to CONTACT, being about 35 times faster.

Dedication

The authors want to dedicate this work to the distinguished civil engineer and University Professor, Dr. Manuel Melis.

Declaration of competing interest

The authors declare that they have no known competing financial interests or personal relationships that could have appeared to influence the work reported in this paper.

Data availability

No data was used for the research described in the article.

Acknowledgments

Grant PRE2018-084067 funded by MCIN/AEI/10.13039/501100011033 and by the EU program "ESF Investing in your future". Grant PID2020-118013RB-C21 funded by MCIN/AEI/10.13039/501100011033. Grant PROMETEO/2021/046 funded by Generalitat Valenciana.

Appendix A

In order to illustrate through an example how the proposed method is implemented, an area of contact with a few elements is modelled through this method. The CONTACT mesh of the potential contact area is shown in Fig. A1, in which the elements that belong to the contact area are numbered and shown in grey colour. Note that this contact area consists of 8 elements distributed in two strips in the $\mathbf{X}_2$-direction. The length of the elements in the $\mathbf{X}_1$-direction is $2a$. Consequently, the half-length of the strips 1 and 2 are $L_1 = 3a$ and $L_2 = 5a$, as shown in Fig. A1.

Following the notation in Eqs. (2) and (6), vector $\mathbf{p}$ is

$$\mathbf{p} = \{ p_{11} \quad p_{21} \quad p_{31} \quad p_{42} \quad p_{52} \quad p_{62} \quad p_{72} \quad p_{82} \}^{\mathrm{T}}, \tag{A2}$$

where the subscript s in p_{es} corresponds to the strip number.

If the contact traction distribution is formulated through an elliptical basis according to Eq. (2), the tractions in the e-th element of the mesh that is in the s-th strip is approached as follows:

$$p_{es} = \alpha_{0s} + \alpha_{1s}\sqrt{1 - \left(\frac{x_{es}}{L_s}\right)^2}. \tag{A3}$$

If Eq. (A3) is implemented in Eq. (A2) through the corresponding parameters for each element, vector $\mathbf{p}$ results

$$\mathbf{p} = \begin{Bmatrix} p_{11} \\ p_{21} \\ p_{31} \\ p_{42} \\ p_{52} \\ p_{62} \\ p_{72} \\ p_{82} \end{Bmatrix} = \begin{Bmatrix} \alpha_{01} + \alpha_{11}\sqrt{1 - \left(\frac{-2a}{3a}\right)^2} \\ \alpha_{01} + \alpha_{11}\sqrt{1 - \left(\frac{0}{3a}\right)^2} \\ \alpha_{01} + \alpha_{11}\sqrt{1 - \left(\frac{2a}{3a}\right)^2} \\ \alpha_{02} + \alpha_{12}\sqrt{1 - \left(\frac{-4a}{5a}\right)^2} \\ \alpha_{02} + \alpha_{12}\sqrt{1 - \left(\frac{-2a}{5a}\right)^2} \\ \alpha_{02} + \alpha_{12}\sqrt{1 - \left(\frac{0}{5a}\right)^2} \\ \alpha_{02} + \alpha_{12}\sqrt{1 - \left(\frac{2a}{5a}\right)^2} \\ \alpha_{02} + \alpha_{12}\sqrt{1 - \left(\frac{4a}{5a}\right)^2} \end{Bmatrix}. \tag{A4}$$

The last equation can be rewritten in the following way:

$$\mathbf{p}=\begin{bmatrix} 1 & \sqrt{1-\left(\frac{-2a}{3a}\right)^2} & 0 & 0 \\ 1 & \sqrt{1-\left(\frac{0}{3a}\right)^2} & 0 & 0 \\ 1 & \sqrt{1-\left(\frac{2a}{3a}\right)^2} & 0 & 0 \\ 0 & 0 & 1 & \sqrt{1-\left(\frac{-4a}{5a}\right)^2} \\ 0 & 0 & 1 & \sqrt{1-\left(\frac{-2a}{3a}\right)^2} \\ 0 & 0 & 1 & \sqrt{1-\left(\frac{0}{5a}\right)^2} \\ 0 & 0 & 1 & \sqrt{1-\left(\frac{2a}{3a}\right)^2} \\ 0 & 0 & 1 & \sqrt{1-\left(\frac{4a}{5a}\right)^2} \end{bmatrix} \begin{Bmatrix} \alpha_{01} \\ \alpha_{11} \\ \alpha_{02} \\ \alpha_{12} \end{Bmatrix} = \mathbf{A}\,\boldsymbol{\alpha}. \tag{A5}$$

from which the calculation of matrix **A** is deduced for this example, giving

$$\mathbf{A}=\begin{bmatrix} 1 & \sqrt{\frac{5}{9}} & 0 & 0 \\ 1 & 1 & 0 & 0 \\ 1 & \sqrt{\frac{5}{9}} & 0 & 0 \\ 0 & 0 & 1 & \frac{3}{5} \\ 0 & 0 & 1 & \sqrt{\frac{5}{9}} \\ 0 & 0 & 1 & 1 \\ 0 & 0 & 1 & \sqrt{\frac{5}{9}} \\ 0 & 0 & 1 & \frac{3}{5} \end{bmatrix}. \tag{A6}$$

Through this simplified case, the number of unknowns is reduced from 8 (the traction in each elements) to 4 (α_{01}, α_{11}, α_{02} and α_{12}). For larger number of elements in a problem with N unknowns, the method allows reducing this number to approximately $2\sqrt{N}$ unknowns.

If the contact traction distribution is formulated through a grade-2 polynomial basis (according to Eq. (6)), vector **p** is approached as follows:

$$\mathbf{p}=\begin{Bmatrix} p_{11} \\ p_{21} \\ p_{31} \\ p_{42} \\ p_{52} \\ p_{62} \\ p_{72} \\ p_{82} \end{Bmatrix} = \begin{Bmatrix} \beta_{01}+\beta_{11}(-2a)+\beta_{21}(-2a)^2 \\ \beta_{01}+\beta_{11}(0)+\beta_{21}(0)^2 \\ \beta_{01}+\beta_{11}(2a)+\beta_{21}(2a)^2 \\ \beta_{02}+\beta_{12}(-4a)+\beta_{22}(-4a)^2 \\ \beta_{02}+\beta_{12}(-2a)+\beta_{22}(-2a)^2 \\ \beta_{02}+\beta_{12}(0)+\beta_{22}(0)^2 \\ \beta_{02}+\beta_{12}(2a)+\beta_{22}(2a)^2 \\ \beta_{02}+\beta_{12}(4a)+\beta_{22}(4a)^2 \end{Bmatrix}. \tag{A7}$$

The last expression can be formulated as

$$\mathbf{p}=\begin{bmatrix} 1 & -2a & (-2a)^2 & 0 & 0 & 0 \\ 1 & 0 & 0 & 0 & 0 & 0 \\ 1 & 2a & (2a)^2 & 0 & 0 & 0 \\ 0 & 0 & 0 & 1 & -4a & (-4a)^2 \\ 0 & 0 & 0 & 1 & -2a & (-2a)^2 \\ 0 & 0 & 0 & 1 & 0 & 0 \\ 0 & 0 & 0 & 1 & 2a & (2a)^2 \\ 0 & 0 & 0 & 1 & 4a & (4a)^2 \end{bmatrix} \begin{Bmatrix} \beta_{01} \\ \beta_{11} \\ \beta_{21} \\ \beta_{02} \\ \beta_{12} \\ \beta_{22} \end{Bmatrix} = \mathbf{B}\,\boldsymbol{\beta}, \tag{A8}$$

from which

$$\mathbf{B} = \begin{bmatrix} 1 & -2a & 4a^2 & 0 & 0 & 0 \\ 1 & 0 & 0 & 0 & 0 & 0 \\ 1 & 2a & 4a^2 & 0 & 0 & 0 \\ 0 & 0 & 0 & 1 & -4a & 16a^2 \\ 0 & 0 & 0 & 1 & -2a & 4a^2 \\ 0 & 0 & 0 & 1 & 0 & 0 \\ 0 & 0 & 0 & 1 & 2a & 4a^2 \\ 0 & 0 & 0 & 1 & 4a & 16a^2 \end{bmatrix}. \tag{A9}$$

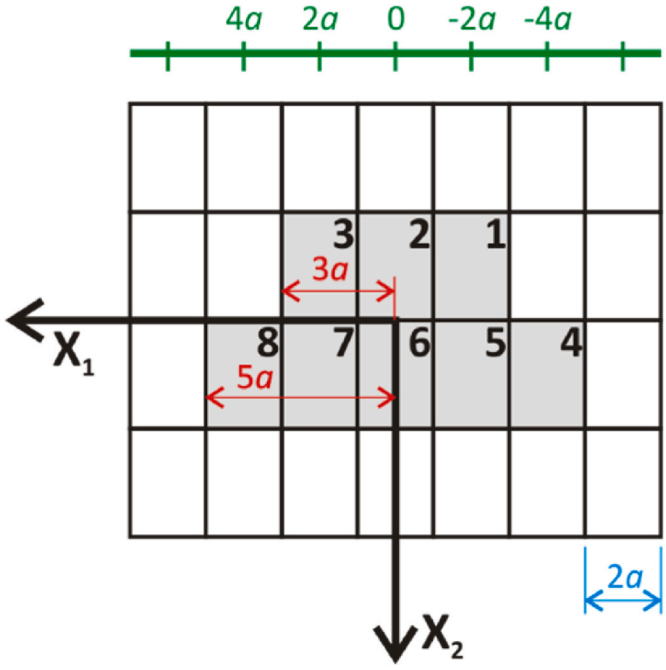

Fig. A1. Simplified mesh of the potential contact area. The grey colour elements correspond with the contact area. The longitudinal dimension of the element ($2a$) is shown in blue, whereas the half-length dimension of the strips (L_s) is drawn in red. The green rule facilitates to know the $\mathbf{X}_1$-coordinate of the element centre (x_c^s).

References

[1] J.J. Kalker, Three-dimensional Elastic Bodies in Rolling Contact, Kluwer Academic Publishers, Dordrecht, 1990.

[2] B. Liu, S. Bruni, Comparison of wheel-rail contact models in the context of multibody system simulation: Hertzian versus non-Hertzian, Veh. Syst. Dyn. 60 (3) (2022) 1076–1096.

[3] E.A.H. Vollebregt, A new solver for the elastic normal contact problem using conjugate gradients, deflation, and an FFT-based preconditioner, J. Comput. Phys. 257 (2014) 333–351.

[4] P. Vila, L. Baeza, J. Martínez-Casas, J. Carballeira, Rail corrugation growth accounting for the flexibility and rotation of the wheelset and the non-Hertzian and non-steady-state effects at contact patch, Veh. Syst. Dyn. 52 (1) (2014) 92–108.

[5] S.Z. Meymand, A. Keylin, M. Ahmadian, A survey of wheel-rail contact models for rail vehicles, Veh. Syst. Dyn. 54 (3) (2016) 386–428, 2016.

[6] J. Piotrowski, H. Chollet, Wheel-rail contact models for vehicle system dynamics including multi-point contact, Veh. Syst. Dyn. 43 (6–7) (2005) 455–483, 2005.

[7] P. Shackleton, S. Iwnicki, Comparison of wheel-rail contact codes for railway vehicle simulation: an introduction to the Manchester Contact Benchmark and initial results, Veh. Syst. Dyn. 46 (1–2) (2008) 129–149.

[8] J.P. Pascal, G. Sauvage, New method for reducing the multicontact wheel/rail problem to one equivalent contact patch, Veh. Syst. Dyn. 20 (1) (1992) 475–489.

[9] J.P. Pascal, The railway dynamic codes: "VOCO", Veh. Syst. Dyn. 22 (1) (1993) 137–139.

[10] A. Alonso, J.G. Giménez, A new method for the solution of the normal contact problem in the dynamic simulation of railway vehicles, Veh. Syst. Dyn. 43 (2) (2005) 149–160.

[11] S. Gu, X. Yang, S. Zhou, S. Lian, Y. Zhou, An innovative contact partition model for wheel/rail normal contact, Wear 366–367 (2016) 38–48.

[12] B. Zhu, J. Zeng, D. Zhang, Y. Wu, A non-Hertzian wheel-rail contact model considering wheelset yaw and its application in wheel wear prediction, Wear (2019) 432–433.

[13] C. Linder, Verschleiss von Eisenbahnrädern mit Unrundheiten, PhD, ETH Zürich, 1997.

[14] J.B. Ayasse, H. Chollet, Determination of the wheel rail contact patch in semi-Hertzian conditions, Veh. Syst. Dyn. 43 (3) (2005) 161–172.

[15] M.S. Sichani, R. Enblom, M. Berg, A novel method to model wheel-rail normal contact in vehicle dynamics simulation, Veh. Syst. Dyn. 52 (12) (2014) 1752–1764, 2014.

[16] M.S. Sichani, R. Enblom, M. Berg, A fast wheel–rail contact model for application to damage analysis in vehicle dynamics simulation, Wear 366–367 (2016) 123–130.

[17] Y. Ye, Y. Sun, D. Shi, B. Peng, M. Hecht, A wheel wear prediction model of non-Hertzian wheel-rail contact considering wheelset yaw: comparison between simulated and field test results, Wear (2021) 474–475.

[18] J. Piotrowski, W. Kik, A simplified model of wheel/rail contact mechanics for non-Hertzian problems and its application in rail vehicle dynamic simulations, Veh. Syst. Dyn. 46 (1–2) (2008) 27–48.

[19] H. Magalhães, et al., Implementation of a non-Hertzian contact model for railway dynamic application, Multibody Syst. Dyn. 48 (1) (2020) 41–78.

[20] Y. Sun, W. Zhai, Y. Ye, L. Zhu, Y. Guo, A simplified model for solving wheel-rail non-Hertzian normal contact problem under the influence of yaw angle, Int. J. Mech. Sci. 174 (2020). Art no. 105554.

[21] Y. Sun, W. Zhai, Y. Guo, A robust non-Hertzian contact method for wheel–rail normal contact analysis, Veh. Syst. Dyn. 56 (12) (2018) 1899–1921.

[22] B. Liu, S. Bruni, E. Vollebregt, A non-Hertzian method for solving wheel–rail normal contact problem taking into account the effect of yaw, Veh. Syst. Dyn. 54 (9) (2016) 1226–1246.

[23] M.S. Sichani, R. Enblom, M. Berg, Comparison of non-elliptic contact models: towards fast and accurate modelling of wheel-rail contact, Wear 314 (1–2) (2014) 111–117.

[24] F. Marques, H. Magalhães, J. Pombo, J. Ambrósio, P. Flores, A three-dimensional approach for contact detection between realistic wheel and rail surfaces for improved railway dynamic analysis, 149Art no, Mech. Mach. Theor. (2020), 103825.

[25] B. An, et al., Assessing the fast non-Hertzian methods based on the simulation of wheel–rail rolling contact and wear distribution, Proc. Inst. Mech. Eng. F J. Rail Rapid Transit 234 (5) (2020) 524–537.

[26] X. Ma, P. Wang, J. Xu, r. Chen, J. Wang, Assessment of non-Hertzian wheel-rail contact models for numerical simulation of rail damages in switch panel of railway turnout, Wear (2019) 432–433.

[27] J.J. Kalker, Review of Wheel-Rail Rolling Contact Theories, vol. 40, American Society of Mechanical Engineers, Applied Mechanics Division, AMD, 1980, pp. 77–92.

[28] J.B. Nielsen, New Developments in the Theory of Wheel/rail Contact Mechanics, PhD, Technical University of Denmark, 1998.
[29] K. Knothe, H. Le The, A contribution to the calculation of the contact stress distribution between two elastic bodies of revolution with non-elliptical contact area, Comput. Struct. 18 (6) (1984) 1025–1033.
[30] H. Reusner, Druckflächenbelastung und Oberflächenverschiebung im Wälzkontakt von Rotationskörpern, PhD, University of Karlsruhe, 1977.
[31] A. Qazi, H. Yin, M. Sebès, H. Chollet, C. Pozzolini, A semi-analytical numerical method for modelling the normal wheel–rail contact, Veh. Syst. Dyn. 60 (4) (2022) 1322–1340.
[32] L. Baeza, D.J. Thompson, G. Squicciarini, F.D. Denia, Method for obtaining the wheel–rail contact location and its application to the normal problem calculation through 'CONTACT', Veh. Syst. Dyn. 56 (11) (2018) 1734–1746.